

基于遗传算法和等效电路模型的窄带通频率选择表面光窗设计方法

姚欣^{1,2,3}, 李浩南^{1,2,3}, 张亚强^{1,2,3}, 牟南历^{1,3}, 董红星^{1,3*}, 张龙^{1,3**}

¹中国科学院上海光学精密机械研究所强激光材料重点实验室, 上海 201800;

²中国科学院大学材料科学与光电技术学院, 北京 100049;

³国科大杭州高等研究院物理与光电工程学院, 江苏 杭州 310024

摘要 提出了一种窄带通频率选择光窗的快速设计方法,该方法结合遗传算法和等效电路模型,能快速准确地给出特定设计目标下光窗的结构参数。该光窗由石英玻璃及镀制在玻璃上下表面的亚波长的金属网栅构成。利用上述方法,可以在几十秒内直接优化出光窗在特定设计目标下的结构参数。与全波仿真相比较,正入射下等效电路模型的准确度高于 93%。利用上述方法对光窗的结构参数进行优化,实现了通带透过系数损失小于 1.5 dB、带外抑制大于 20 dB、品质因子高于 26 的性能,同时光窗保持一定的可见光透过率且具有极化不敏感性。结果表明,该方法能快速有效地设计窄带通频率选择光窗。

关键词 材料; 带通频率选择表面; 可见光透过率; 金属网栅; 等效电路法; 遗传算法

中图分类号 O441

文献标志码 A

doi: 10.3788/CJL202249.0603004

1 引言

频率选择表面(FSS)由二维周期性排列的结构单元组成,可以实现对特定电磁波波段的带通或带阻^[1-3]。由于它对电磁波具有特殊调控能力,FSS引起了广泛的研究兴趣。近几十年来,FSS被用于降低飞行器的雷达散射截面,减少室内环境中的无线信号干扰,以及保护敏感的电子设备,使其免受干扰^[4-6]。近些年来,频率选择表面也被加载在光学窗口上,除了能实现带内电磁信号的透过和带外电磁波的屏蔽,也可以维持可见光的高透性^[7-13],因而可用于光学/雷达多模导引头罩、机载多模通信探测窗口和车载透明天线等方面^[14-19]。然而,由于频率选择表面的设计通常需要用全波仿真和参数扫描来获得最优参数,这一过程要耗费大量的时间和计算资源,因此简化频率选择表面的设计过程对于带通频率选择光窗的研究十分必要。

对于网栅和介质这类结构,Simovski 课题组推导出准确度较高的解析公式来计算这类结构在等效

电路中的集总参数^[20]。因此等效电路模型可以替代全波仿真来计算由金属网栅和介质构成的频率选择表面的透过系数。然而,等效电路模型仅仅给出了结构参数和透过系数的关系,通常还需要通过参数扫描获得合适的结构参数。因此,快速获得符合设计目标的结构参数十分重要。Behdad 课题组用巴特沃夫滤波器的设计方法结合等效电路法,有效地反推出由金属网栅和介质构成的二阶窄带通频率选择表面的结构参数^[21],但是反推过程仍旧存在查表、反推结构参数等过程,不能直接给出结构参数。对于这类多参数的优化问题,遗传算法是一种快速有效的解决方法^[22-24]。遗传算法是一种基于进化和自然选择概念的优化算法,通过选择、变异和交叉等操作模拟自然选择的过程,筛选出最优个体,相比滤波器的设计方法,能极大地降低计算时间,从而更快地得到特定设计目标下的结构参数。因此,结合遗传算法和等效电路法两者的优点,可以快速有效地设计频率选择光窗。

基于以上讨论,本文提出了一种快速设计窄带

收稿日期: 2021-07-21; 修回日期: 2021-08-16; 录用日期: 2021-08-24

通信作者: *hongxingd@siom.ac.cn; **Lzhang@siom.ac.cn

通频率选择光窗的方法,该方法结合遗传算法和等效电路模型,能快速准确地给出特定设计目标下光窗的结构参数。该光窗由石英玻璃及镀制在玻璃上下表面的微金属网栅构成,用等效电路模型计算出网栅和石英玻璃复合结构的结构参数和透过系数之间的关系,然后通过遗传算法优化出符合设计目标且较优的结构参数。为了验证设计方法的有效性,我们将优化得到的结果和全波仿真结果进行对比,计算出等效电路模型的准确度高于 93%。结构参数优化后的光窗具有通带透过系数的损失小于 1.5 dB、带外抑制大于 20 dB、品质因子高于 26 的性能,同时保持一定的可见光透过率且具有极化不敏感性。因此,该设计方法能快速准确地设计窄带通频率选择光窗,极大地简化了网栅和介质结构频

率选择表面的设计过程。

2 基本原理

2.1 结构组成

本文用一种由上下两层金属网栅、中间一层介质构成的窄带通频率选择光窗的结构来验证设计方法的有效性。这一结构中的介质层作为高 Q 谐振器,与金属网栅耦合后,对特定频点电磁波有高透的效果。该结构由三层构成,如图 1(a)所示,其中中间一层的介质层为透明的石英玻璃,相对介电常数 $\epsilon_r = 3.7$,厚度为 h_1 。上下两层为导电良好的金属银网栅,电导率为 6.3×10^7 S/m,为了简化设计,将上下两层设为一致,周期均为 D ,网栅线宽均为 w_1 ,厚度为 h_2 。

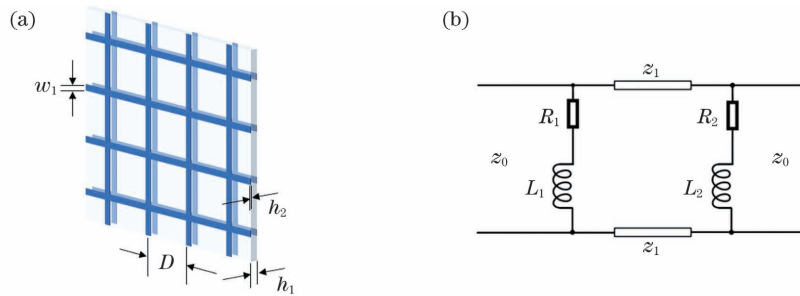


图 1 窄带通频率选择光窗。(a)结构示意图;(b)等效电路图

Fig. 1 Narrow bandpass frequency selective optical window. (a) Structural diagram; (b) equivalent circuit

2.2 等效电路模型

金属网栅和介质可用等效电路模型来分析,其中最重要的是得到等效电路集总参数的电阻、电容和电感。当金属网栅的周期 D 远小于入射波的波长,并且网栅线宽 w_1 远小于网栅的周期 D 时,金属网栅的电容可以忽略不计。图 1(b)给出了光窗的等效电路图,其中 Z_0 是空气的特征阻抗, Z_1 是等效为传输线的介质层的阻抗, $R_{1,2}$ 为上下两层金属网栅的等效电阻, $L_{1,2}$ 为上下两层金属网栅的等效电感。金属网栅的等效电阻为

$$R = R_s \frac{S}{A} = \frac{S}{\sigma h_2 A}, \quad (1)$$

式中: R_s 是金属的方阻; S 是一个周期单元的面积; σ 是银的电导率; h_2 是银网栅的厚度; A 是一个周期单元内金属网栅所占的面积。

对于横电(TE)和横磁(TM)极化的入射波,网栅的电抗^[20]分别近似为

$$X_g^{\text{TE}} = \frac{\eta_{\text{eff}}}{2} \alpha, \quad (2)$$

$$X_g^{\text{TM}} = \frac{\eta_{\text{eff}}}{2} \alpha \left(1 - \frac{k_0^2 \sin^2 \theta}{k_{\text{eff}}^2} \right), \quad (3)$$

式中: $\eta_{\text{eff}} = \sqrt{\mu_0 / \epsilon_0 \epsilon_{\text{eff}}}$ 是介质基板的有效阻抗,其中 μ_0 是真空中磁导率, ϵ_0 是真空中介电常数, ϵ_{eff} 是介质的有效介电常数,当金属网栅位于空气和介质的分界面时, $\epsilon_{\text{eff}} = (\epsilon_r + 1) / 2$, ϵ_r 为介质的相对介电常数; $k_{\text{eff}} = k_0 \sqrt{\epsilon_{\text{eff}}}$ 是有效波数; k_0 是真空中波数; θ 是入射角, TM 极化波与入射角 θ 有关; α 是网格系数,表达式为

$$\alpha = \frac{k_{\text{eff}} D}{\pi} \ln \left[\frac{1}{\sin(\pi w_1 / 2D)} \right]. \quad (4)$$

依据以上电阻和电抗的近似估计,可得到 FSS 的阻抗为

$$Z_g^{\text{TE, TM}} = R + jX_g^{\text{TE, TM}}. \quad (5)$$

单层介质的 ABCD 矩阵^[20]可写为

$$\begin{bmatrix} A_1 & B_1 \\ C_1 & D_1 \end{bmatrix} = \begin{bmatrix} \cosh(jv h_1) & Z_c^{\text{TE, TM}} \sinh(jv h_1) \\ \frac{\sinh(jv h_1)}{Z_c^{\text{TE, TM}}} & \cosh(jv h_1) \end{bmatrix}, \quad (6)$$

式中: h_1 是介质层厚度;波数 k_d 的垂直分量 $v =$

$k_d \cos \theta'$, 其中 θ' 是入射角为 θ 时的折射角, $k_d = \omega \sqrt{\epsilon_0 \epsilon_r \mu_0}$, ω 是入射电磁波的角频率, 依据折射定律计算得到

$$\theta' = \arcsin\left(\frac{\sin \theta}{\sqrt{\epsilon_r}}\right). \quad (7)$$

在(6)式中, $Z_c^{\text{TE, TM}}$ 是包含斜入射极化效果的特性阻抗:

$$Z_c^{\text{TE}} = \frac{(\eta_0 / \sqrt{\epsilon_r})}{\cos \theta'}, \quad (8)$$

$$Z_c^{\text{TM}} = \frac{\eta_0}{\sqrt{\epsilon_0}} \cos \theta', \quad (9)$$

式中: η_0 是自由空间的固有波阻抗。整个 FSS 的透过系数可以通过每层的 ABCD 矩阵相乘得到。图 1(a)所示结构总的 ABCD 矩阵可写为

$$\begin{bmatrix} A_2 & B_2 \\ C_2 & D_2 \end{bmatrix} = \begin{bmatrix} 1 & 0 \\ \frac{1}{Z_1^{\text{FSS}}} & 1 \end{bmatrix} \begin{bmatrix} A_1 & B_1 \\ C_1 & D_1 \end{bmatrix} \begin{bmatrix} 1 & 0 \\ \frac{1}{Z_2^{\text{FSS}}} & 1 \end{bmatrix}, \quad (10)$$

式中: Z_1^{FSS} 为第一层金属网栅的阻抗, 可将第一层金属网栅的线宽 ω_1 和周期 D 代入(5)式中计算得到; Z_2^{FSS} 为第二层金属网栅的阻抗, 可将第二层金属网栅的线宽 ω_1 和周期 D 代入(5)式中计算得到。

透过系数(S_{11})和反射系数(S_{21})与 $A_2 B_2 C_2 D_2$ 参数的关系为

$$S_{11} = \frac{(A_2 + B_2/Z_0^{\text{TE, TM}}) - (Z_0^{\text{TE, TM}} C_2 + D_2)}{(A_2 + B_2/Z_0^{\text{TE, TM}}) + (Z_0^{\text{TE, TM}} C_2 + D_2)}, \quad (11)$$

$$S_{21} = \frac{2}{(A_2 + B_2/Z_0^{\text{TE, TM}}) + (Z_0^{\text{TE, TM}} C_2 + D_2)}, \quad (12)$$

式中: 对于 TE 和 TM 极化, 自由空间的固有波阻抗为

$$Z_0^{\text{TE}} = \frac{\eta_0}{\cos \theta}, \quad (13)$$

$$Z_0^{\text{TM}} = \eta_0 \cos \theta. \quad (14)$$

2.3 遗传算法

带通频率选择光窗是一个多目标的优化问题, 适应度函数需要同时考虑透过峰频率、透过峰透过率和带外抑制。带通频率选择光窗的设计目标有: 1) 透过峰频率接近设计目标; 2) 透过峰透过系数高; 3) 带外抑制好。考虑到以上几点, 适应度函数写为

$$F =$$

$$a_1 |f_{\max} - f_0| + a_2 |S_{21, \max}| + a_3 |S_{21, \min} - \Delta_{\min}|. \quad (15)$$

适应度函数由三项分别乘以其权重组成, 其中第一项是对透过峰频率与目标透过峰频率之间误差的评价, 变量 f_{\max} 为透过峰的频率(单位为 GHz), f_0 为优化目标的透过频率(单位为 GHz), a_1 为透过峰的频率相对设计目标的误差的权重。当透过峰频率 f_{\max} 越接近 f_0 , 第一项越小。第二项是对透过峰透过系数的评价, 变量 $S_{21, \max}$ 为透过峰透过系数(单位为 dB), a_2 为透过率的权重。 $S_{21, \max}$ 越接近 0, 第二项越小。第三项是对带外抑制的评价, $S_{21, \min}$ 为透过峰相邻透过系数的极小值(单位为 dB), Δ_{\min} 为设计目标的透过系数的极小值(单位为 dB), a_3 为其的权重。 $S_{21, \min}$ 越接近 Δ_{\min} , 第三项越小。依据计算经验, 当取 $a_1 = 1, a_2 = a_3 = 5$ 时, 优化得到的结果与设计目标的误差均保持在可以接受的范围内。

遗传算法的优化流程如图 2 所示。依据自变量的取值范围随机建立初始种群, 依据等效电路模型和设计目标编写适应度函数。将初始种群代入适应度函数, 若达到收敛的要求, 则输出满足要求的自变量。若未达到收敛的要求, 再通过遗传算法的选择及交叉和变异算子, 产生下一代种群, 重复上述步骤直到满足收敛的要求, 最终输出优化后的最符合设计目标的自变量。

自变量的取值受实际加工能力和设计目标的限制。受实际加工能力的限制, 介质厚度 h_1 的精度为 $\pm 0.1 \text{ mm}$, 网栅周期 D 和网栅线宽 ω_1 的精度为 $\pm 1 \mu\text{m}$ 。结构对可见光的总透过率^[25]为

$$T = T_m T_d \geq T_{m, \min} T_d = \left(\frac{D - 2\omega_1}{D}\right)^2 T_d = \left(1 - \frac{2\omega_1}{D}\right)^2 T_d, \quad (16)$$

式中: T_m 是双层网栅对可见光的透过率; T_d 是介质层的透过率; $T_{m, \min}$ 是 T_m 的最小值。单层网栅的透过率为一个周期内未被网栅覆盖的面积与一个周期的面积之比, 考虑到双层网栅在实际加工过程中存在位错, 因此一个周期内未被覆盖的最小面积为 $(D - 2\omega_1)^2$ 。网栅的线宽和周期之比 ω_1/D 越低, 透过率越大, 同时伴随着带外屏蔽效果的降低。因此可以依据设计目标选择合适的线宽与周期之比。本文取 $\omega_1/D \leq 0.05$, 此时结构的总透过率将大于 $81\% T_d$ 。

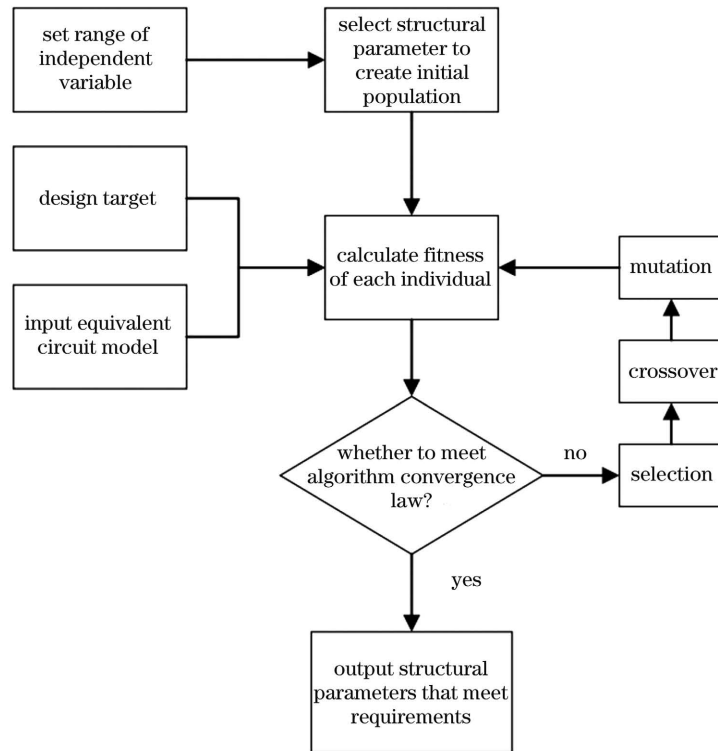


图 2 频率选择表面设计优化流程图

Fig. 2 Flow chart of FSS design and optimization

3 分析与讨论

为了验证优化方法的准确性和有效性,选取两组设计目标,经遗传算法优化后输出两组结构参数,再将结构参数分别代入等效电路模型和全波仿真软件 CST Studio 中,得到其透过系数曲线,最后计算了等效电路模型计算的结构透过系数相对全波仿真结果的误差,用以验证等效电路模型的准确性,同时计算了算法优化得到的结构参数中的透过系数与设计目标的误差,用以验证优化算法的有效性。

两组设计目标如下:目标透过频率 f_0 分别设定为 12 GHz 和 13 GHz,透过系数的极小值 Δ_{\min} 设定为 -25 dB。考虑到趋肤深度,取 $h_2 = 300$ nm。算法优化后均可在半分钟之内得到设计目标对应的两组结构参数,对应的结构设计分别为 design-I 和 design-II,其最小透过率如表 1 所示,可见优化结构的透过率均不小于 $0.81T_d$ 。

将这两组结构参数代入全波仿真软件 CST Studio 和等效电路模型中,得到对应的 S_{21} 曲线(图 3)和相关参数(表 2)。其中, f_0 是目标透过峰的频点, f_M 是利用等效电路模型算出的透过峰的频点, f_S 是利用 CST 软件算出的透过峰的频点, $S_{21,M,\max}$ 是利用等效电路模型计算出来的透过峰的

透过系数, $S_{21,S,\max}$ 是利用 CST Studio 计算出来的透过峰的透过系数, $S_{21,M,\min}$ 是利用等效电路模型计算出来的透过系数的极小值, $S_{21,S,\min}$ 是利用 CST Studio 计算出来的透过系数的极小值, Q 是透过峰的品质因子,为共振峰的中心频点与半峰全宽之比。由图 3 和表 2 可见, design-I 和 design-II 的透过峰接近设计目标,实现了窄带通和较高的带外抑制,全波仿真结果显示其透过峰频率分别为 11.86 GHz 和 12.95 GHz,与设计目标 12 GHz 和 13 GHz 的误差均低于 0.2 GHz,误差较小,透过峰的透过系数损失分别为 1.38 dB 和 1.42 dB,带外抑制均大于 20 dB,品质因子分别为 26.91 和 28.13。

以全波仿真作为参照,等效电路模型的准确度^[26]定义为

$$A_{\text{accuracy}} = \frac{\sum_{f_L}^{f_H} |S_{21,S}| - \sum_{f_L}^{f_H} |S_{21,S} - S_{21,M}|}{\sum_{f_L}^{f_H} |S_{21,S}|} \times 100\%, \quad (17)$$

式中: $S_{21,S}$ 和 $S_{21,M}$ 分别是全波仿真和等效电路模型得到的透过系数; f_H 是比较的频率范围内的最大频率; f_L 是比较的频率范围内的最小频率。依据(17)式,在电磁波正入射到 design-I 和 design-II 上

时,前述等效电路模型的准确度均高于 93%。可以看出,等效电路模型可以较为准确地计算其透过系数。

此外,还分别用等效电路模型和全波仿真的方法计算了电磁波斜入射到 design-I 和 design-II 的情况,具体计算了当斜入射角为 0°~60°时 TE 和 TM 极化下 8~26 GHz 频段的透过系数。利用 (17) 式计算出等效电路模型得到的透过系数相对全波仿真结果的准确度,结果如表 3 所示。由表 3 可见,在 0°~30°斜入射下,等效电路模型相对全波仿真的准确度大于 88%,准确度较高。在 30°~60°大角度斜入射下,等效电路模型的准确度略有下降,但

准确度仍维持在 76%以上。因此,等效电路模型可以较为准确地计算出不同斜入射角和 TE/TM 极化下的入射波的透过系数曲线。图 4 展示了电磁波以 0°~60°斜入射到 design-I 和 design-II 上时 TE 和 TM 极化下全波仿真计算的透过率曲线,可见对于 0°~30°斜入射角,该结构的透过峰均保持在 12 GHz 附近,透过率几乎不变且对 TE/TM 极化不敏感。对于大角度的入射,该结构的透过峰有明显的偏移(图 4)。图 5 为利用全波仿真计算的不同极化角下正入射到 design-I 结构和 design-II 结构的透过率。由于网栅中心对称,在 0°~45°极化角下,该结构的透过率曲线保持不变。因此该结构对极化角不敏感。

表 1 遗传算法优化的结构参数

Table 1 Structural parameters optimized by genetic algorithm

Design	f_0/GHz	$w_1/\mu\text{m}$	h_1/mm	$D/\mu\text{m}$	$T_{m,\min}/\%$
I	12	44	5.9	880	81
II	13	40	5.4	800	81

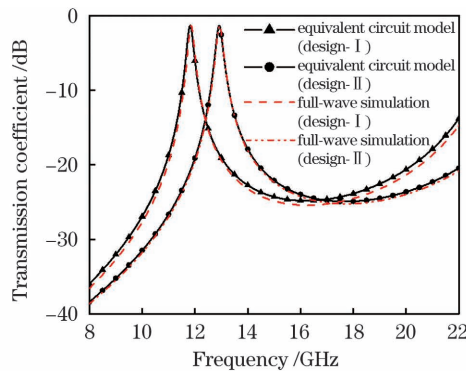


图 3 由全波仿真和等效电路模型算出的 design-I 结构和 design-II 结构的透过系数

Fig. 3 Transmission coefficients of design-I and design-II using proposed EC model and full-wave simulation

表 2 遗传算法优化的结果以及全波仿真的结果对比

Table 2 Comparison of results optimized by genetic algorithm and full-wave simulation

Design	f_0/GHz	f_M/GHz	f_S/GHz	$S_{21,M,\max}/\text{dB}$	$S_{21,S,\max}/\text{dB}$	$S_{21,M,\min}/\text{dB}$	$S_{21,S,\min}/\text{dB}$	Q
I	12.00	11.82	11.86	-1.31	-1.38	-24.84	-25.43	26.91
II	13.00	13.00	12.95	-1.42	-1.42	-24.95	-25.00	28.13

表 3 等效电路模型计算的透过率相对全波仿真结果的误差

Table 3 Relative error of transmissivity obtained by EC model with respect to that by full-wave simulation

Design	Polarization state	Incident angle of 0°	Incident angle of 10°	Incident angle of 20°	Incident angle of 30°	Incident angle of 40°	Incident angle of 50°	Incident angle of 60°	unit: %
I	TE	93.22	93.62	94.88	96.94	94.25	85.92	79.78	
	TM	93.22	92.52	90.78	88.42	85.51	83.43	76.41	
II	TE	96.76	97.82	97.22	98.20	92.79	87.03	79.22	
	TM	96.76	96.60	92.39	91.26	89.77	84.94	77.57	

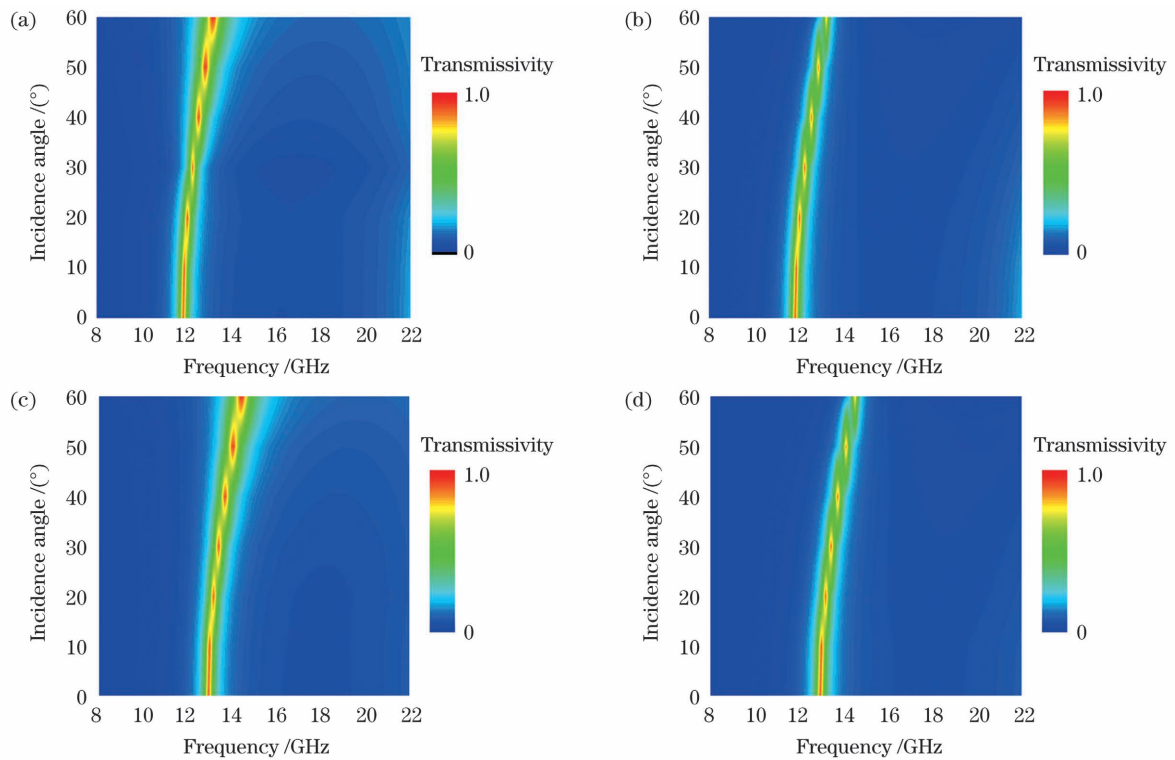


图 4 全波仿真计算出的 design-I 结构和 design-II 结构的透过率。(a) design-I, TE 极化; (b) design-I, TM 极化; (c) design-II, TE 极化; (d) design-II, TM 极化

Fig. 4 Transmissivities of design-I and design-II using full-wave simulation. (a) design-I, TE-polarized; (b) design-I, TM-polarized; (c) design-II, TE-polarized; (d) design-II, TM-polarized

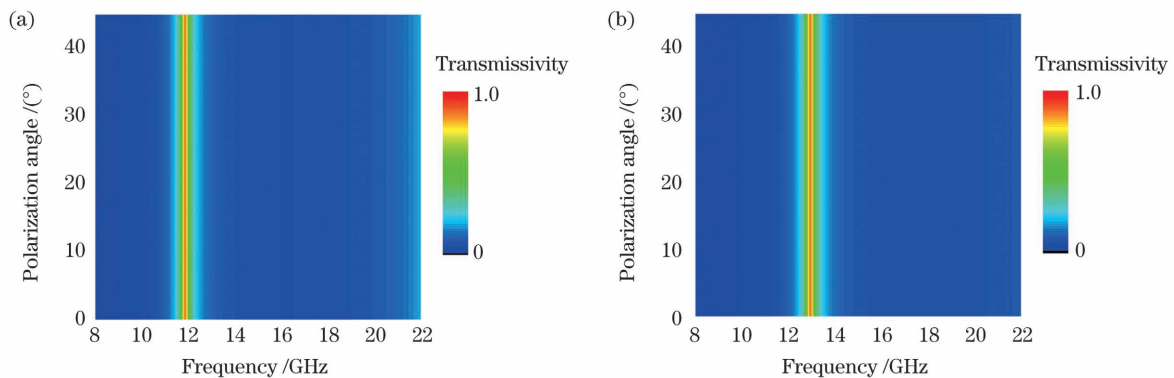


图 5 全波仿真计算出的不同极化角下正入射到 design-I 结构和 design-II 结构的透过率。(a) design-I; (b) design-II

Fig. 5 Transmissivities of design-I and design-II for normal incident waves with different polarization angles using full-wave simulation. (a) design-I; (b) design-II

4 结 论

提出了一种快速设计窄带通频率选择光窗的方法,该方法结合遗传算法和等效电路模型,能快速准确地给出特定设计目标下光窗的结构参数。在不同斜入射角和 TE/TM 极化下,对比了全波仿真和等效电路模型计算出的透过系数曲线,计算出正入射下等效电路模型结果相对 CST 全波仿真结果的准确度大于 93%, $0^{\circ}\sim 30^{\circ}$ 斜入射下准确度大于 88%,

且结构的通带透过系数损失均小于 1.5 dB,带外抑制大于 20 dB,同时可见光透过率不小于 $0.81T_d$,结构对极化角不敏感。因此,该方法能快速准确地优化出介质和网栅复合结构在特定设计目标下的结构参数,极大地缩短了金属网栅类频率选择表面的设计时间,为频率选择表面的设计提供了便利。

参 考 文 献

- [1] Wu T K. Frequency selective surfaces [M] //

- Encyclopedia of RF and Microwave Engineering. Hoboken: John Wiley & Sons, Inc., 2005.
- [2] Mittra R, Chan C H, Cwik T. Techniques for analyzing frequency selective surfaces-a review [J]. Proceedings of the IEEE, 1988, 76(12): 1593-1615.
- [3] Abbaspour-Tamijani A, Sarabandi K, Rebeiz G M. Antenna-filter-antenna arrays as a class of bandpass frequency-selective surfaces [J]. IEEE Transactions on Microwave Theory and Techniques, 2004, 52(8): 1781-1789.
- [4] Sung G H H, Sowerby K W, Neve M J, et al. A frequency-selective wall for interference reduction in wireless indoor environments[J]. IEEE Antennas and Propagation Magazine, 2006, 48(5): 29-37.
- [5] Kiani G I, Ford K L, Olsson L G, et al. Switchable frequency selective surface for reconfigurable electromagnetic architecture of buildings [J]. IEEE Transactions on Antennas and Propagation, 2010, 58(2): 581-584.
- [6] Abadi S M A M H, Li M, Behdad N. Harmonic-suppressed miniaturized-element frequency selective surfaces with higher order bandpass responses [J]. IEEE Transactions on Antennas and Propagation 2014, 62(5): 2562-2571.
- [7] Cao W, Singh R, Zhang C H, et al. Plasmon-induced transparency in metamaterials: active near field coupling between bright superconducting and dark metallic mode resonators [J]. Applied Physics Letters, 2013, 103(10): 101106.
- [8] Ra'Di Y, Asadchy V S, Tretyakov S A. One-way transparent sheets[J]. Physical Review B, 2014, 89(7): 075109.
- [9] Lu Z, Liu Y, Wang H, et al. Optically transparent frequency selective surface based on nested ring metallic mesh [J]. Optics Express, 2016, 24(23): 26109-26118.
- [10] Sharma S K, Zhou D G, Luttgen A, et al. A micro copper mesh-based optically transparent triple-band frequency selective surface [J]. IEEE Antennas and Wireless Propagation Letters, 2019, 18(1): 202-206.
- [11] Han Y, Liu Y M, Jin P, et al. Optical-transparent Wi-Fi bandpass mesh-coated frequency selective surface [J]. Electronics Letters, 2014, 50(5): 381-383.
- [12] Taylor P S, Parker E A, Batchelor J C. An active annular ring frequency selective surface [J]. IEEE Transactions on Antennas and Propagation, 2011, 59(9): 3265-3271.
- [13] Zhuo H Y, Liu Z Q, Peng W, et al. Design and application of electromagnetic shielding of optical detection system [J]. Infrared and Laser Engineering, 2020, 49(6): 20190412.
- 卓红艳, 刘志强, 彭文, 等. 光学探测系统电磁屏蔽设计与应用 [J]. 红外与激光工程, 2020, 49(6): 20190412.
- [14] Zhang Y Q, Dong H X, Ye Q, et al. FAST perimeter security monitoring system low frequency broadband high efficiency electromagnetic shielding light window [J]. Chinese Journal of Lasers, 2021, 48(3): 0316001.
- 张亚强, 董红星, 叶青, 等. FAST 周界安防监控系统低频-宽带高效电磁屏蔽光窗 [J]. 中国激光, 2021, 48(3): 0316001.
- [15] Perruisseau-Carrier J. Graphene for antenna applications: opportunities and challenges from microwaves to THz [C] // 2012 Loughborough Antennas & Propagation Conference (LAPC), November 12-13, 2012, Loughborough, UK. New York: IEEE Press, 2012: 13255996.
- [16] Deng F, Yi X Q, Wu W J. Design and performance of a double-layer miniaturized-element frequency selective surface [J]. IEEE Antennas and Wireless Propagation Letters, 2013, 12: 721-724.
- [17] Li B, Shen Z X. Angular-stable and polarization-independent frequency selective structure with high selectivity [J]. Applied Physics Letters, 2013, 103(17): 171607.
- [18] Chen X, Gao J S, Fang C Y, et al. Deformable frequency selective surface structure with tuning capability through thermoregulating [J]. Optics Express, 2015, 23(12): 16329-16338.
- [19] Xu Y, Gao J S, Xu N X, et al. A novel broadband bi-mode active frequency selective surface [J]. AIP Advances, 2017, 7(5): 055012.
- [20] Luukkonen O, Simovski C, Granet G, et al. Simple and accurate analytical model of planar grids and high-impedance surfaces comprising metal strips or patches [J]. IEEE Transactions on Antennas and Propagation, 2008, 56(6): 1624-1632.
- [21] Momeni Hasan Abadi S M A, Behdad N. Inductively-coupled miniaturized-element frequency selective surfaces with narrowband, high-order bandpass responses [J]. IEEE Transactions on Antennas and Propagation, 2015, 63(11): 4766-4774.
- [22] Weile D S, Michielssen E. Genetic algorithm optimization applied to electromagnetics: a review [J]. IEEE Transactions on Antennas and Propagation, 1997, 45(3): 343-353.
- [23] Shim H, Lee J, Lee F Y, et al. Optimal design of frequency selective surface by genetic algorithm [J]. International Journal of Precision Engineering and Manufacturing, 2010, 11(5): 725-732.

- [24] Campos A L P S, Martins A M, Almeida Filho V A. Synthesis of frequency selective surfaces using genetic algorithm combined with the equivalent circuit method [J]. *Microwave and Optical Technology Letters*, 2012, 54(8): 1893-1897.
- [25] Martin A, Castel X, Himdi M, et al. Influence of the mesh dimensions on optically transparent and active antennas at microwaves[C]//2016 International Symposium on Antennas and Propagation (ISAP), October 24-28, 2016, Okinawa, Japan. New York: IEEE Press, 2016: 16601762.
- [26] Hossain M I, Nguyen-Trong N, Sayidmarie K H, et al. Equivalent circuit design method for wideband nonmagnetic absorbers at low microwave frequencies [J]. *IEEE Transactions on Antennas and Propagation*, 2020, 68(12): 8215-8220.

Design Method of Optical Window with Narrow Bandpass Frequency Selective Surface Based on Genetic Algorithm and Equivalent Circuit Model

Yao Xin^{1,2,3}, Li Haonan^{1,2,3}, Zhang Yaqiang^{1,2,3}, Mou Nanli^{1,3},
Dong Hongxing^{1,3*}, Zhang Long^{1,3*}

¹Key Laboratory of Materials for High-Power Laser, Shanghai Institute of Optics and Fine Mechanics, Chinese Academy of Sciences, Shanghai 201800, China;

²College of Materials Science and Opto-Electronic Technology, University of Chinese Academy of Sciences, Beijing 100049, China;

³School of Physics and Opto-Electronic Engineering, Hangzhou Institute for Advanced Study, University of Chinese Academy of Sciences, Hangzhou, Jiangsu 310024, China

Abstract

Objective An optical window with a bandpass frequency selective surface (FSS) can transmit microwave signals at the desired frequency band and shield out-of-band signals, while transmitting visible light. However, designing frequency selective surfaces often require parameter scanning and full-wave simulation to obtain structural parameters corresponding to the desired design goals. This process is complicated and computational, so it is necessary to simplify the design. In this paper, a method is proposed to quickly design narrow bandpass optical transparent frequency selective surfaces. The method combines the genetic algorithm and the equivalent circuit (EC) model, and can quickly and accurately output the structural parameters of optical transparent windows under the desired design goals, which is verified by full-wave simulation. The loss of transmission peaks is less than 1.5 dB at the desired frequency, the out-of-band suppression is larger than 20 dB, the quality factors of transmission peaks are larger than 26, the visible light transmittance is acceptable, and the structure is not sensitive to polarization angles.

Methods In this paper, the structure of an optical transparent bandpass FSS is proposed to verify the effectiveness of the design method. The structure is composed of a glass layer with silver grids plated on its upper and lower surfaces, as shown in Fig. 1(a). The equivalent circuit models of the metal grid and the dielectric layer are given (Fig. 1(b)) to calculate the total scattering parameters. The design goals of the band-pass electromagnetic shielding optical window are: 1) the frequency of the transmission peak is close to the design goal; 2) the transmission peak is high; 3) the out-of-band suppression is big enough. Considering the above points, the fitness function is written as Eq. (15). The overall optimization process is shown in Fig. 2. It can be seen that the initial population is established according to the value range of the independent variable. And the adaptive function is determined by the equivalent circuit model and the design goal. Appropriate values are screened out through the adaptive function, and the structural parameters conforming to the convergence rule are output.

Results and Discussions Through the optimization by genetic algorithm and the EC method, two sets of structural parameters corresponding to the goals of design I and design II are obtained (Table 1). Compare the curves under two sets of structural parameters calculated by CST Studio software and equivalent circuit model (Fig. 3 and Table 2), it can be seen that the transmission peaks of design-I and design-II are close to the design goals,

achieving a narrow passband and high out-of-band suppression. The full-wave simulation results show that the frequencies of transmission peaks are located at 11.86 GHz and 12.95 GHz, and the transmissivity losses are 1.38 dB and 1.42 dB, respectively. Besides, the out-of-band shielding is greater than 20 dB, and the quality factors of transmission peaks are 26.91 and 28.13, respectively. Moreover, the accuracy of the EC relative to the full-wave simulation when calculating the transmissivities of design- I and design- II at the oblique incidence angle of 0° – 60° for TE or TM polarization, is calculated by formula (17), and the results are shown in Table 3. It can be seen from Table 3 that the accuracy of the EC model relative to the full-wave simulation is high. Finally, the transmissivities of design- I and design- II at 0° – 45° polarization angle (Fig. 5) are simulated, and it can be seen that the structure is not sensitive to polarization angle.

Conclusions In summary, this paper proposes an accurate and fast design method to design a narrow bandpass optical transparent FSS. Two structural parameters are optimized under the design goals by this method and are verified to be close to the design goals by full-wave simulation, with the losses of transmission peaks less than 1.5 dB at the desired frequency, the out-of-band suppression larger than 20 dB, the quality factors of transmission peaks larger than 26, the visible light transmittance acceptable, and the structure not sensitive to polarization angles. In addition to optimizing the structural parameters of the bandpass optical transparent FSS at the desired transmission frequency point, this design method can also be used to optimize design goals of different optical transmittances and dielectric materials, or a multi-layer FSS that consists of media and metal grids. Therefore, this method can effectively optimize the structural parameters of the FSS composed of dielectric and grid structures under desired design goals, greatly reduces the design time of the metal grid type FSS, and provides convenience for the design of the FSS.

Key words materials; bandpass frequency selective surface; visible light transmissivity; metal mesh; equivalent circuit method; genetic algorithm